Supporting Information

Self-Location of Acceptors as 'Isolated' or 'Stacked' Energy Traps in a Supramolecular Donor Self-assembly: A Strategy to Wavelength Tunable FRET Emission

Ayyappanpillai Ajayaghosh,* Chakkooth Vijayakumar, Vakayil K. Praveen, S. Santhosh Babu and Reji Varghese

Photosciences and Photonics Unit, Chemical Sciences and Technology Division,

Regional Research Laboratory,

CSIR, Trivandrum 695 019 (India)

1. Experimental Section

General

The solvents and the reagents were purified and dried by usual methods prior to use. Reagents purchased from commercial suppliers were used as such. All melting points were determined with a Mel-Temp-II melting point apparatus and are uncorrected. ^{1}H and ^{13}C NMR spectra were recorded on a 300 MHz Bruker Advance DPX Spectrometer. FT-IR spectra were recorded on a Shimadzu IRPrestige-21 Fourier Transform Infrared Spectrophotometer. MALDI-TOF mass spectrometry was conducted on a Perspective Biosystems Voyager DE PRO MALDI-TOF mass spectrometer using α-Cyano-4-hydroxy cinnamic acid as the matrix.

2. Synthesis and characterization

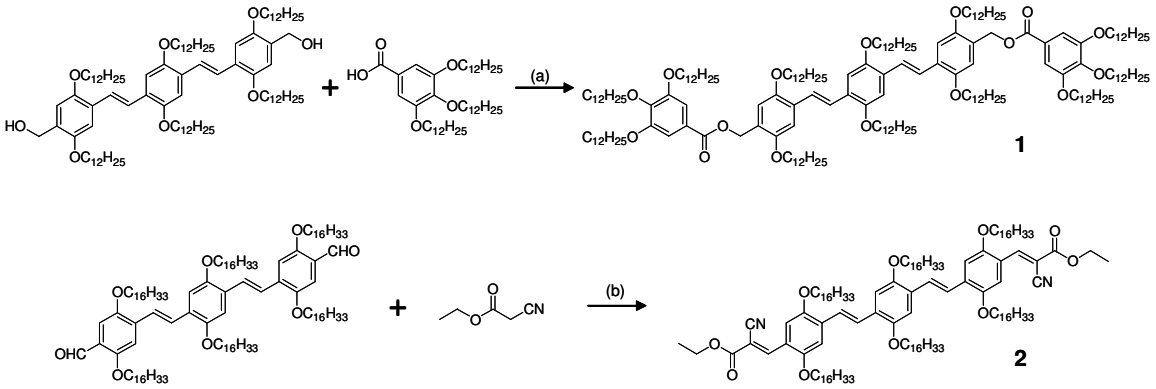

Scheme S1. Synthesis of **1** and **2**. Reagents and conditions: (a) DCC (2 equiv.), DMAP, DCM (dry), 0 °C - rt, 4h, 96%; (b) NH_4OAC, CH_3COOH, toluene, 80 °C, 4h, 95%.

Syntheses of **1** and **2** were achieved as per Scheme 1. The OPV bisaldehyde and the corresponding bisalcohol were prepared as reported earlier.[1] The OPV bisalcohol (0.5 mmol) and the O-alkylated gallic acid derivative (1.1 mmol) were reacted in dry dichloromethane in the presence of DCC and DMAP for 4 h. The reaction mixture was filtered and the solvent evaporated. The crude mixture was then purified by eluting through a silica column (100-200 mesh) using chloroform-hexane (1: 3) mixture. Compound **2** was obtained by treating the OPV aldehyde (0.5 mmol) with ethyl cyanoacetate (1.1 mmol) in dry toluene in the presence of catalytic amount of acetic acid and ammonium acetate at 80 °C for 4 h. The solvent was evaporated, residue dissolved in chloroform and extracted with water. The organic layer was dried over anhydrous sodium sulphate and the solvent was evaporated. The residue was dissolved in chloroform and precipitated with methanol to get the pure product.

1: Yield 96%. m.p. 80-82 °C. ^{1}H NMR (300 MHz, $CDCl_3$, TMS) δ (ppm): 0.78-0.82 (m, 36H), 1.19 (s, 192H), 1.35-1.44 (m, 24H), 1.62-1.81 (m, 24H), 3.90-4.00 (m, 24H), 5.31 (s, 4H), 6.91 (s, 2H), 7.07 (s, 4H), 7.22 (s, 8H), 7.40 (s, 4H). ^{13}C NMR (75 MHz, $CDCl_3$, TMS): 14.11, 22.68, 26.07, 26.13, 26.22, 29.37, 29.43, 29.49, 29.59, 29.70, 31.93, 62.27, 67.77, 69.00, 69.16, 69.59, 73.50, 108.06, 109.51, 110.41, 114.76, 116.24, 123.18, 123.74, 124.76, 124.96, 127.28, 127.91, 150.46, 151.00, 151.39, 152.79, 166.38. FT-IR (KBr) ν_{max} 690, 723, 758, 804, 855, 899, 932, 966, 1024, 1068, 1120, 1209, 1250, 1333, 1383, 1427, 1464, 1508, 1591, 1717, 2850, 2920 cm^{-1}; MALDI-TOF m/z 2760.40 (calculated mass = 2760.41).

2: Yield 95%; m.p. 107-109 °C; ^{1}H NMR (300 MHz, $CDCl_3$, TMS) δ (ppm) 0.85-0.88 (m, 18H), 1.24 (s, 96H), 1.42-1.52 (m, 18H), 1.84-1.89 (m, 12H), 4.07-4.09 (m, 12H), 4.34-4.41 (q, 4H), 7.16. (s, 4H), 7.49-7.54 (d, 2H), 7.60-7.66 (d, 2H), 7.98 (s, 2H), 8.78 (s, 2H); ^{13}C NMR ($CDCl_3$, 75 MHz, TMS) δ (ppm) 14.32, 14.43, 22.90, 26.34, 26.46, 26.53, 29.46, 29.59, 29.69, 29.74, 29.95, 32.15, 62.49, 69.38, 69.59, 100.14, 109.78, 110.93, 111.88, 116.95, 120.37, 123.34, 127.12, 127.73, 134.74, 148.82, 150.74, 151.63, 154.08, 163.46; FT-IR (KBr): ν_{max} 719, 763, 802, 854, 961, 1024, 1049, 1091, 1165, 1213, 1240, 1294, 1346, 1365, 1394, 1429, 1467, 1506, 1571, 1726, 2214, 2848, 2916, 2956 cm^{-1}; MALDI-TOF MS m/z = 1969.73 (calculated mass = 1969.68).

3. Description of Experimental Techniques

3.1. Gelation

Gelation studies were carried out in glass vials of 1 cm diameter. A weighed amount of the compound in an appropriate solvent was placed in the vial, which was sealed and heated until the compound was dissolved. The solution was allowed to cool. The gel formation was confirmed by the failure of the content to flow by inverting the glass vial. Repeated heating and cooling confirmed the thermal reversibility of gelation. The critical gelator concentration (CGC) is determined from the minimum amount of gelator required for the formation of a stable gel at room temperature.

3.2. Electronic Spectral Measurements

Electronic absorption spectra were recorded on a Shimadzu UV-3101 PC NIR scanning spectrophotometer and the emission spectra were recorded on a SPEX-Flourolog F112X spectrofluorimeter. Temperature dependent studies were carried out with a thermistor directly attached to the wall of the cuvette holder.

3.3. Fluorescence Lifetime Measurements

Fluorescence lifetimes were measured using IBH (FluoroCube) time-correlated picosecond single photon counting (TCSPC) system. Solutions were excited with a pulsed diode laser (<100 ps pulse duration) at a wavelength of 375 nm (NanoLED-11) with a repetition rate of 1 MHz. The detection system consists of a microchannel plate photomultiplier (5000U-09B, Hamamatsu) with a 38.6 ps response time coupled to a monochromator (5000M) and TCSPC electronics (DataStation Hub including Hub-NL, NanoLED controller and preinstalled Fluorescence Measurement and Analysis Studio (FMAS) software). The fluorescence lifetime values were determined by deconvoluting the instrument response function with biexponential decay using DAS6 decay analysis software. The quality of the fit has been judged by the fitting

parameters such as χ^2 (<1.2) as well as the visual inspection of the residuals. All measurements were carried out in a 1mm cuvette using a front face sample holder (5000U-04).

3.4. X-Ray Diffraction Studies

Concentrated solutions of the samples were prepared by dissolving it in chloroform by heating. The hot solution was poured on to a glass plate and allowed to evaporate slowly to get good films. X-ray diffractograms of the dried films were recorded on a Phillips Diffractometer using Ni filtered Cu Kα radiation.

3.5. Fluorescent Microscopic Studies

Fluorescent microscopic images were recorded on a Nikon EpiFluorescent Microscope TE300 using UV light (330-380 nm) as the excitation source. Samples were prepared by drop casting decane solution (concentration of the donor was kept at 3 x 10^{-4} M and concentration of the acceptor varied from 0-20 mol%) on a glass slide followed by slow evaporation.

3.6. Atomic Force Microscopic Studies

Atomic Force Microscopy images were recorded under ambient conditions using a Digital Instrument Multimode Nanoscope IV operating in the tapping mode regime. Micro-fabricated silicon cantilever tips (MPP-11100-10) with a resonance frequency of 299 kHz and a spring constant of 20-80 Nm^{-1} were used. The scan rate varied from 0.5 to 1.5 Hz. AFM section analyses was done offline. Samples for the imaging were prepared by drop casting the decane solution at the required compositions of donor and acceptor on freshly cleaved mica. Concentration of the donor was kept at 1 x 10^{-5} M and concentration of the acceptor varied from 0-20 mol%. Blank experiments with neat solvents on mica sheet were carried out to eliminate the possibility of any artifacts, prior to the measurements of the samples.

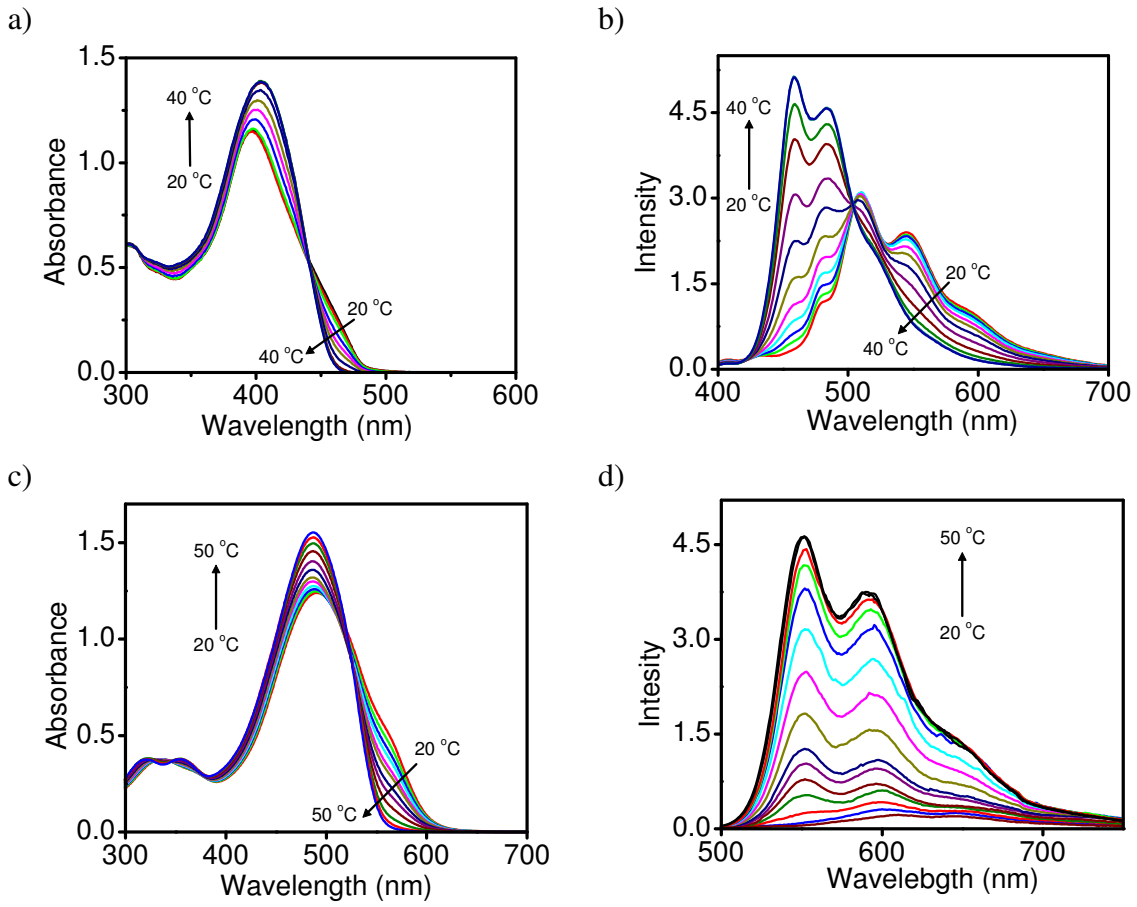

Figure S1. Temperature dependent absorption spectra of (a) **1**, (c) **2** and fluorescence spectra of (b) **1**, (d) **2** in decane that reveal the thermoreversible aggregation of **1** and **2** (c = 3 × 10^{-4} M, l = 1mm, λ_{ex} = 380 nm for **1**, λ_{ex} = 480 nm for **2**).

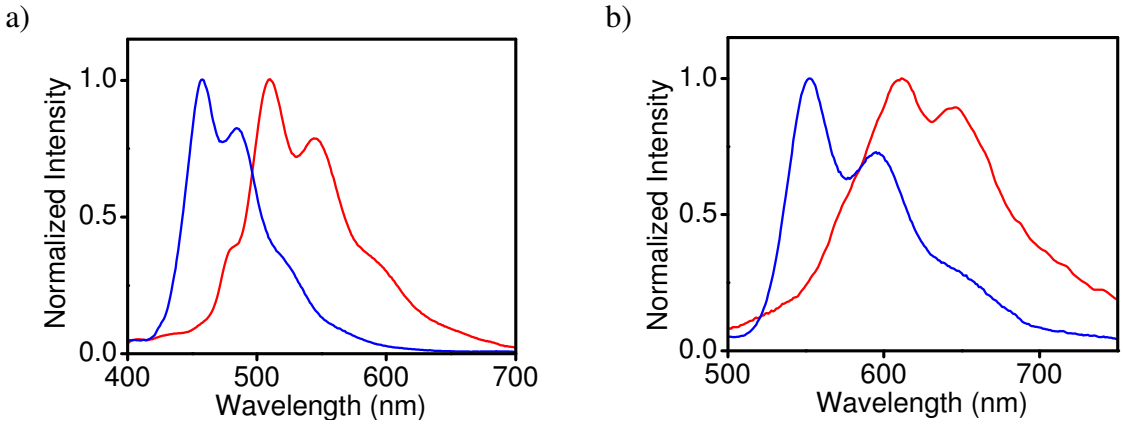

Figure S2. Fluorescence spectra of (a) **1** and (b) **2** in the solution state (blue, c = 1 × 10^{-6} M) and in the gel state (red, c = 3 × 10^{-4} M) in decane at 20 °C (l = 1mm, λ_{ex} = 380 nm for **1**, λ_{ex} = 480 nm for **2**).

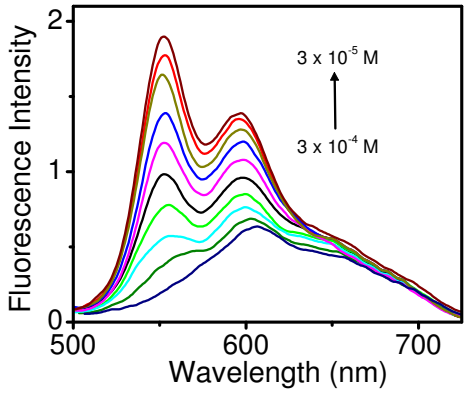

Figure S3. Concentration dependent fluorescence spectra of **2** in decane at 20 °C that shows the aggregation at higher concentrations. (l = 1mm, λ_{ex} = 480 nm)

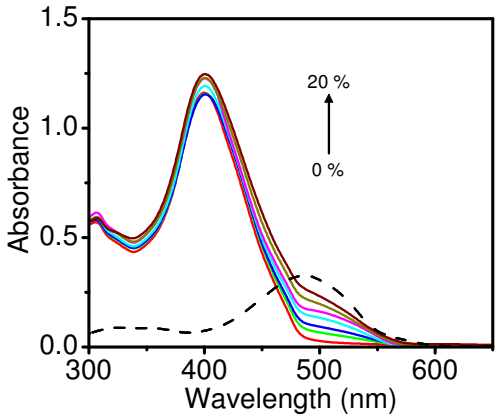

Figure S4. Absorption spectral changes of **1** on addition of 0-20 mol% of **2** in decane at 20 °C. Dashed line shows the absorption spectrum of **2** alone having same concentration that of the acceptor present in co-assembly containing 20 mol% of **2**. From this figure it is clear that the acceptor has very low absorbance at 380 nm at which the donor is excited for FRET experiments.

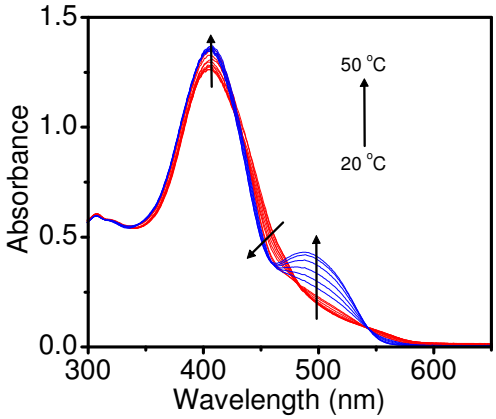

Figure S5. Temperature dependent absorption changes of **1** in presence of 20 mol% **2** in decane. Red lines indicate the spectral changes from 20-40 °C which corresponds to the melting of the donor aggregates. Blue lines indicate the spectral changes from 40-50 °C which corresponds to the melting of the acceptor aggregates formed within the self-assembly of the donor.

Temperature dependent UV/Vis absorption studies showed two transitions upon heating the decane solution of the coassembly (donor conc. = 3×10^{-4} M) containing 20 mol% of **2** (Figure S5). The increase in the intensity of the absorption around 400 nm and the decrease of the shoulder band at 470 nm at 20-40 °C, correspond to the disruption of the donor scaffold. The second transition observed at 40-50 °C with an increase in the absorption around 491 nm corresponds to the melting of the acceptor aggregates.

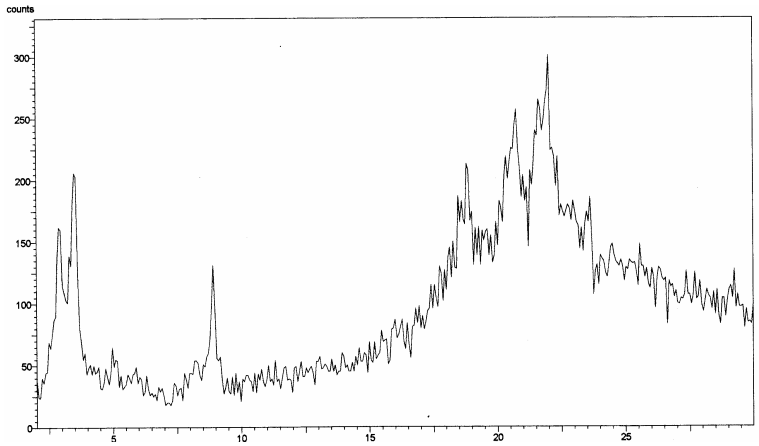

Figure S6. Powder XRD pattern of the donor **1**

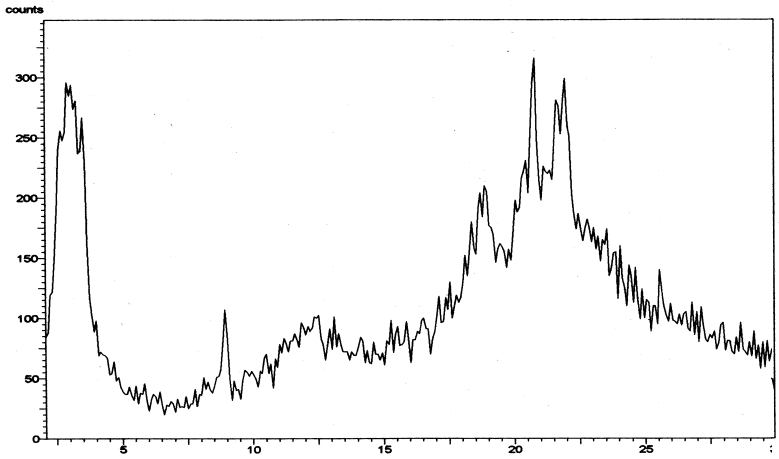

Figure S7. Powder XRD of **1** in the presence of 10 mol% of **2**.

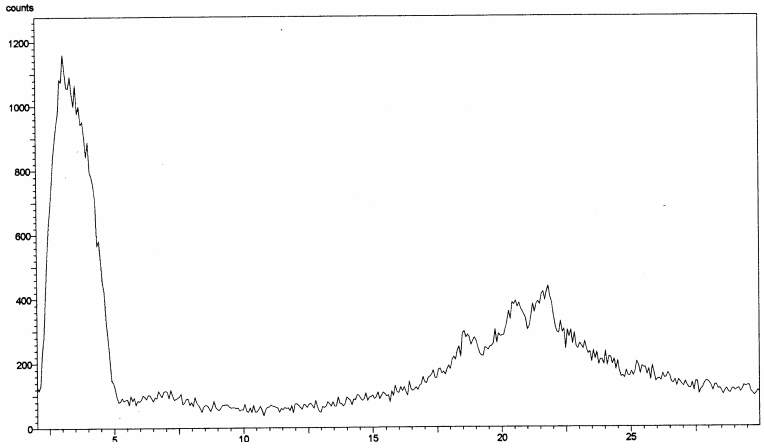

Figure S8. Powder XRD of **1** in the presence of 20 mol% of **2**.

X-ray diffraction patterns of **1** showed sharp reflections corresponding to the *d*-spacing of 30.15, 25.30, 9.93, 4.70, 4.29 and 3.78 Å which are indications of π-stacked lamellar packing of the molecules (Figure S6). Absence of the sharp reflections, particularly at 9.93 Å, the broadening of the peaks at the short and the wide angle regions and the shift in the π-stacking distance from 3.78 to 4.07 Å with 20 mol% of the acceptor indicates the disruption of the continuous lamellar packing of **1** as a result of the intercalation of **2** (Figure S8).

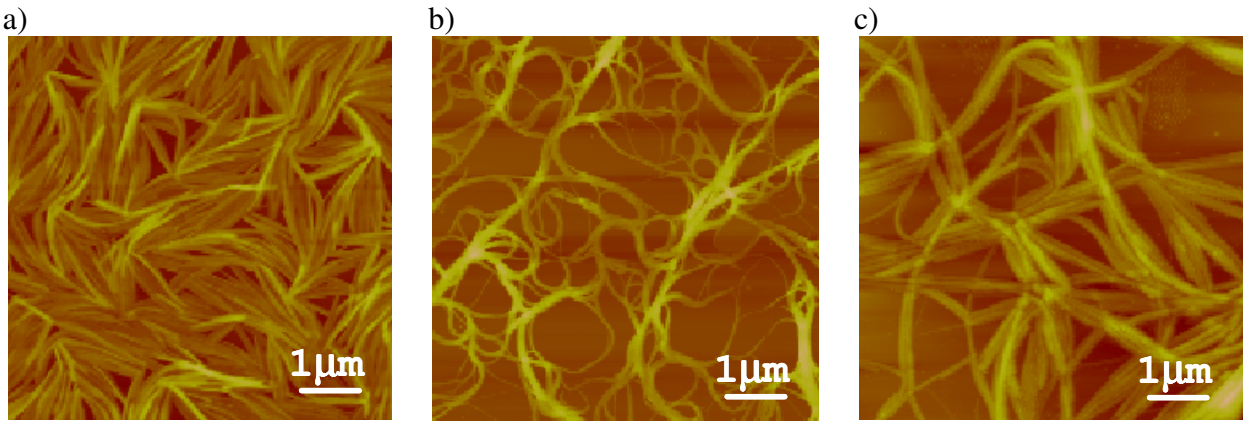

Figure S9. AFM tapping mode height images of (a) **1** alone (b) **2** alone (c) coassembly of **1** with 20 mol% of **2** (donor conc. = 1×10^{-5} M in decane), recorded at same magnification.

AFM images of **1**, **2** and the coassemblies revealed the formation of micrometer sized extended structures with distinct morphological features. For example, the morphology of **1** exhibits short fibrous texture, several of which are aligned together to form bundles (Figure S9a). The individual strands are a few micrometers in length, 100-160 nm in width and 8-20 nm in height which are not entangled. On the other hand, **2** forms entangled structures of infinite length having 40-200 nm width and 5-50 nm height (Figure S9b). Interestingly, the coassembly of **1** with 20 mol% of **2** showed morphological features of both compounds (100-300 nm width and 5-50 nm height, Figure S9c). These observations confirmed the coassembly of the acceptor within the donor scaffold.

4. Gelation Studies

Table S1: Critical gelator concentration in mg/mL (mM) of **1** and **2.**

Sl. No.	Solvent	**1** **mg/mL (mM)**	**2** **mg/mL (mM)**
1.	n-Decane	1.0 (0.36)	1.6 (0.81)
2.	n-Hexane	1.2 (0.43)	2.3 (1.06)
3.	Cyclohexane	1.5 (0.54)	4.2 (2.12)
4.	Methyl cyclohexane	2.6 (0.94)	4.3 (2.17)
5.	p-Xylene	7.5 (2.7)	10.5 (5.29)

5. Calculation of Spectral Overlap Integral

The spectral overlap integral $J(\lambda)$ of the donor emission and the acceptor absorption was calculated using equation 1.[2]

$$J(\lambda) = \frac{\int_0^\infty F_D(\lambda)\, \varepsilon_A(\lambda)\, \lambda^4\, d\lambda}{\int_0^\infty F_D(\lambda)\, d\lambda} \qquad \text{- - - - - - - - (1)}$$

Where $F_D(\lambda)$ is the fluorescence intensity of the donor in the wavelength range λ to $\lambda+\Delta\lambda$, $\varepsilon_A(\lambda)$ is the extinction coefficient of the acceptor at λ.

6. Calculation of Efficiency of Energy Transfer

The efficiency of energy transfer was estimated from the donor fluorescence-quenching profiles by using the equation 2.[2]

$$\text{Efficiency of energy transfer} = \quad 1 - \frac{I_{DA}}{I_D} \qquad \text{----------(2)}$$

Where I_D (3.0964) and I_{DA} (0.0508) emission intensities of the donor in the absence and presence of acceptor respectively.

7. Calculation of Energy transfer rate constant

Rate of energy transfer (k_{ET}) was determined by using the following equation, which provides a lower limit for energy transfer rate.[3]

$$k_{ET} = \quad \frac{Q_{max} - 1}{\tau_D} \qquad \text{-------(3)}$$

Where $Q_{max} = I_D/I_{DA}$, is the maximum quenching observed in the fluorescence titration studies. τ_D is the lifetime of the donor. The fluorescence decay profiles of donor, **1** showed a biexponential decay with lifetime values τ_1 = 1.96 ns (α_1 = 60.58) and τ_2 = 4.33 ns (α_2 = 39.42). Here τ is the lifetime and α is the corresponding amplitude of the decay component of the donor. So in order to determine the rate of energy transfer we used average life time of the donor $<\tau>$ = 3.36 ns, by using the following equation (equation 4).[2]

$$<\tau> = \frac{\alpha_1\tau_1^2 + \alpha_2\tau_2^2}{\alpha_1\tau_1 + \alpha_2\tau_2} \qquad \text{---------(4)}$$

8. References:

(1) (a) Ajayaghosh, A.; George, S. J. *J. Am. Chem. Soc.* **2001**, *123*, 5148. (b) George, S. J.; Ajayaghosh, A. *Chem.-Eur. J.* **2005**, *11*, 3217.

(2) Lakowicz, J. R. *Principles of Fluorescence Spectroscopy*; Kluwer Academic/Plenum Publishers: New York, **1999**.

(3) (a) Beckers, E. H. A.; van Hal, P. A.; Schenning, A. P. H. J.; El-ghayoury, A.; Peeters, E.; Rispens, M. T.; Hummelen, J. C.; Meijer, E. W.; Janssen, R. A. J. *J. Mater. Chem.* **2002**, *12*, 2054. (b) Neuteboom, E. E.; Beckers, E. H. A.; Meskers, S. C. J.; Meijer, E. W.; Janssen, R. A. J. *Org. Biomol. Chem.* **2003**, *1*, 198.